International Journal of Pharmaceutics 512 (2016) 213–218

Contents lists available at ScienceDirect

International Journal of Pharmaceutics

journal homepage: www.elsevier.com/locate/ijpharm

Synthesis and physicochemical properties of polyacrylamide nanoparticles as photosensitizer carriers

M.S. Gualdesi[a], C.I. Alvarez Igarzabal[b], J. Vara[a], C.S. Ortiz[a,*]

[a] Departamento de Farmacia, Facultad de Ciencias Químicas, Universidad Nacional de Córdoba, Argentina
[b] Departamento de Química Orgánica, Facultad de Ciencias Químicas, Universidad Nacional de Córdoba. IMVIB-CONICET, Argentina

ARTICLE INFO

Article history:
Received 23 May 2016
Received in revised form 18 August 2016
Accepted 24 August 2016
Available online 26 August 2016

Keywords:
Photosensitizers
Nanocarriers
Photodynamic therapy
Phenazines derivatives
Phenothiazines derivatives

ABSTRACT

At present, polyacrylamide nanoparticles are attractive to drug delivery. However, some physicochemical characteristics of these nanoparticles still need to be further improved in practice. Polyacrylamide nanoparticles with an average size of 80 nm and a zeta potential of −30 mV were synthesized and used as photosensitizer carriers. The new monobrominated derivatives and parent compounds were the photosensitizers for the photodynamic therapy loaded in the nanocarrier.

The physicochemical characterization of the prepared nanoparticles, drug loading, the ability to generate singlet oxygen and chemical stability were investigated.

The novel tested nanoparticles exhibited a loading percentage of between 80 and 99%, higher generation of singlet oxygen and good stability in comparison with the corresponding starting reagent.

According to these results, the novel polyacrylamide nanoparticles are excellent candidates for drug vehiculization.

1. Introduction

Photodynamic Therapy (PDT) is a minimally invasive therapeutic modality used for the treatment of a variety of cancerous and non-cancerous diseases. This therapeutic alternative utilizes light-sensitive molecules called photosensitizers (PSs), which are drugs activated by light of a specific wavelength. Photodynamic sensitizers produce reactive oxygen species that in biological systems trigger a cascade of biochemical responses that result in cell death (Pereira Rosa et al., 2015; Rodrigues et al., 2013; Yuri Nagata et al., 2012; Weijer et al., 2015).

Nanoparticles (NPs) are innovative biological applications, which have been extensively used due to their advantages of material- and size- dependent physics and chemical interactions with the cellular systems. Nanosized materials have emerged as effective systems for therapeutic applications (Ferreira dos Santos et al., 2015; Maya et al., 2013; Saha et al., 2015).

Depending on the type of nanocarrier and the mode of attachment or loading of PS onto it, the use of NPs in conjunction with PDT may impede the premature release of PS and potential inactivation of the drug by plasma components, thus preventing its nonspecific accumulation and reducing overall photosensitivity. The NPs protect the loaded PSs from degradation, enhance their transport, prevent their aggregation, and represent an emerging technology in the field of PDT that can overcome most of the limitations of classic PS. The properties of PS mainly depend on chemical and physical parameters, such as lipophilicity, type and number of charged groups, charge-to-mass ratio, and type and number of ring and core substituents. Most of the classical PSs have poor solubility under physiological conditions, undesirable pharmacokinetics, and low cellular selectivity.

Although the hydrophobic characteristic of PSs can allow them to penetrate the cell membrane and locate in the photosensitive subcellular compartment, highly hydrophobic PSs could form aggregates in aqueous solution, particularly under physiological milieu, which, in turn, could affect their photophysical and photokilling properties due to their inadequate pharmacokinetics (Paszko et al., 2011; Swarnalatha Lucky et al., 2015).

Positively charged PSs are efficiently taken up by cells and accumulate intracellularly to concentrations higher than in the environment. They are electrostatically attracted by the predominantly negatively charged components of the plasma and

* Corresponding author.
E-mail address: crisar@fcq.unc.edu.ar (C.S. Ortiz).

http://dx.doi.org/10.1016/j.ijpharm.2016.08.051
0378-5173/

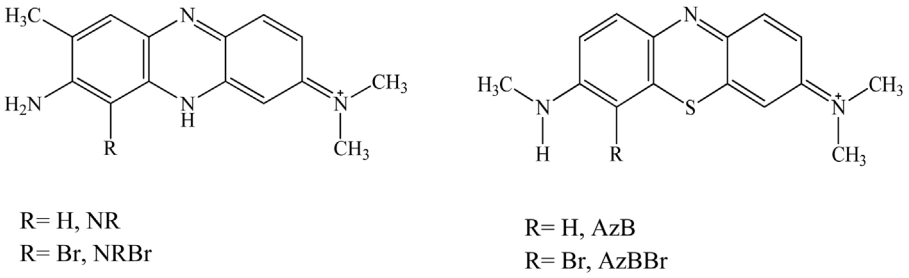

Fig. 1. Chemical structure of PSs.

mitochondrial membranes. The critical force driving such positively charged molecules inside cells and mitochondria is the transmembrane potential.

Many products can behave like PSs and new ones are regularly discovered; however, very few have made it to clinical trial. Each of the currently commercially available PS has specific characteristics, but none of them is an ideal agent (Master et al., 2013; Yano et al., 2011).

There are several vehiculization strategies, such as liposomes, polymeric micelles, polymer nanoparticles, gold nanoparticles, and colloidal silica-based nanoparticles that are well known for improving the therapeutic capability of the PS in aqueous systems. The most commonly used synthetic polymers employed to prepare nanoparticles for drug vehiculization are biodegradable (Li and Huh, 2014). NPs composed of biodegradable materials have the ability to move through capillaries to target cells and evade immune responses which can prematurely eliminate the PS from the body.

Recent accelerated biodegradation studies demonstrated the biodegradability of the polyacrylamide nanomaterials (Kolya and Tripathy, 2014). Polyacrylamide (PAA) nanoparticles are promising vehicles for photodynamic therapy. The PAA nanoparticle matrix, generally a porous hydrogel protects the embedded active form of PS from enzymatic or environmental degradation and permits singlet oxygen and other kinds of reactive oxygen species (ROS) diffusion through the pores. In view of the above-mentioned facts, we developed a nanocarrier strategy using biocompatible polymers to incorporate NR, NRBr, AzB and AzBBr.

The four PSs shown in Fig. 1 have very similar structures. Neutral Red (NR) is a phenazine-based dye, which is very useful as a biological probe, and has been widely utilized for various purposes in many biological systems, such as the staining of cellular particles and the intracellular pH indicator. In addition, NR has been used as a PS in PDT and good results have been obtained (Fischer et al., 2005; Singh et al., 1999).

The new phenazine cationic dye, monobrominated Neutral Red (NRBr), was synthesized and characterized in our laboratory. This compound proved to have the potential to be used as a PS because it presents less aggregation in different solvents in comparison with the parent compound. The improved photoproperties exhibited by NRBr were accompanied by significant increases in the photoantimicrobial action compared to NR (Urrutia et al., 2015). This newly synthesized phenazine dye has shown a slight discoloration in the studied experimental conditions. In this context, photosensitizer-loaded nanocarriers can have the capability to reduce this effect modifying the physicochemical properties (Urrutia et al., 2015).

The phenothiazine, Azure B (AzB), is a positively charged compound used as a phototherapeutic agent due to its appropriate biological, chemical, photochemical and photophysical properties; therefore, AzB and the new derivatives, monobrominated Azure B (AzBBr), which were synthesized and characterized in our work group, are candidate agents to produce photocytotoxicity in biological media (Fig. 1) (Montes de Oca et al., 2013). The introduction of bromine atom into the chromophoric system caused an increase in the lipophilicity. Moreover, the *in vitro* photodynamic activity against LM-2 murine mammary carcinoma cells demonstrated that the photocitoxicity of AzBBr remained unchanged or decreased. The lower efficiency to inactivate cultured tumor cells may be attributed to the aggregation effects of phenothiazinium derivatives (Montes de Oca et al., 2013).

The photodynamic inactivation in cell suspensions of *Candida albicans* observed for AzB and AzBBr derivatives can be associated with a different distribution of agents in the cell, mainly due to the number and location of the positive charge on the PS. Although studies of photodynamic action mechanism indicated that photoinactivation of *C. albicans* cells induced by phenothiazinium derivatives produce singlet molecular oxygen, a contribution of other reactive oxygen species cannot be discarded in the photoinactivation (Alvarez et al., 2014). Besides, the entrapment of these PSs could offer therapeutic advantages in comparison to free PS active agents since it could prevent different adverse effects.

2. Experimental section

2.1. Materials

NR (3-amino-7-dimethylamino-2-methyl phenazine hydrochloride) and AZB (3-(Dimethylamino)-7-(methylamino)phenothiazine-5-ium chloride) were purchased from Sigma Chemical Co, and its purity was confirmed by RP-HPLC (> 98%). NRBr and AzBBr were synthesized in our laboratory according to the procedure previously described (Montes de Oca et al., 2013; Urrutia and Ortiz, 2013).

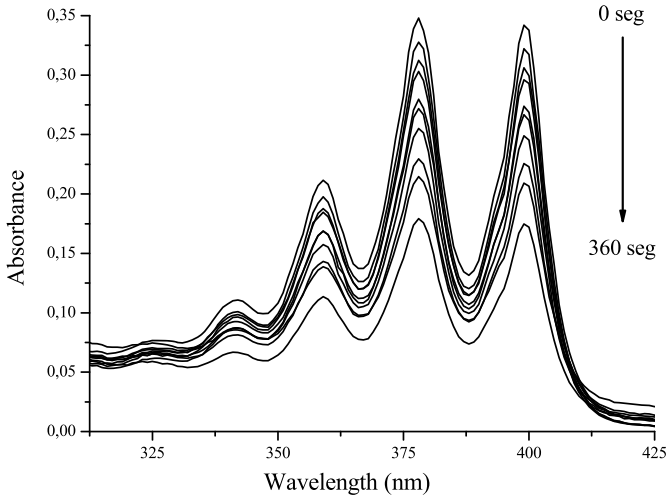

Fig. 2. UV–vis absorbance spectra of ABDA in solution with AzB irradiated at different times.

Acrylamide, N,N,N',N'-tetraethylmethylenediamine (TEMED), ammonium persulfate (APS), polyethylene glycol dodecyl ether (Brij 30), 3-(acryloyloxy)-2-hydroxypropyl methacrylate (AHM), dioctyl sulfosuccinate (AOT), 3-(aminopropyl) methacrylamide (APMA) and 9,10- Anthracenediyl-bis (methylene)dimalonic acid (ABDA) were purchased from Sigma-Aldrich. Hexane, DMSO, ethanol, methanol and acetonitrile were obtained from Sintorgan. Purification by dialysis was performed with membranes of cellulose ester (MWCO 50 KDa; SpectrumLabs).

Phosphate-buffered saline (PBS, 10 mM pH 7.4) solution was prepared using sodium chloride, potassium chloride, sodium hydrogen phosphate dihydrate and potassium dihydrophosphate. The pH was determined by a CRISON GLP 21 pH-meter, using a combined glass electrode. All the chemicals were of the highest purity commercially available (Cicarelli) and the solutions were prepared using ultrapure water from Milli-Q® purification system.

2.2. Instrumentation

Absorption spectra were carried out at room temperature with a Cary 60 UV–vis (Agilent Technologies) spectrophotometer between 200 and 800 nm, using a 1 cm length quartz cell. All experiments were carried out at least twice with consistent results. The RP-HPLC measurements were performed on an Agilent Series 1100 chromatograph equipped with an autosampler, a column thermostat, an UV–vis detector and a reversed-phase C18 Phenomenex® column (4.6 mm × 250 mm, 5 μm) with a guard column. The column temperature was set at 25 °C and the flow rate at 1.0 mL/min. The mobile phases and the samples prepared in them were filtered through a Millipore® Type FH filter (0.45 μm pore size). Subsequently, the mobile phases were vacuum degassed. Data were produced by means of a Peak Simple Chromatography Data System®

The droplet size, polydispersity index (PDI), as well as zeta potential of the purified NPs were determined at 25 °C, using a Beckman Coulter® DelsaTM Nano C Particle Analyser with a He-Ne laser (633 nm), a scattering angle of 165°, a viscosity of 0.8878 Pa s and a refractive index of 1.3328. The samples were appropriately diluted with water before their analysis. A minimum of three measurements were taken and averaged for each determination.

2.3. Synthesis of polyacrylamide nanoparticles

The NPs used in this study were prepared through inverse microemulsion polymerization. Several parameters, such as reaction time and amount of activator and initiator, were assessed in order to optimize the formation of the NPs. Once these conditions were experimentally determined, the NPs were prepared. In summary, hexane (45 mL) was added to a dried 100 mL reaction flask and stirred under a constant purge of nitrogen during 5 min. Suitable amounts of surfactants AOT (1.6 g) and Brij 30 (3.1 g) were added to the reaction flask and stirring was continued under nitrogen protection for 20 min. Acrylamide (monomer, 711 mg), APMA (monomer, 89 mg) and biodegradable AHM (crosslinker, 428 mg) were dissolved in phosphate buffered saline (2 mL) (PBS, pH 7.4) in a glass vial by sonication to obtain an uniform solution. This solution was then added to the hexane reaction mixture and stirred at 500 rpm for another 20 min at 22 °C. Polymerization was initiated by adding equal volume of TEMED and freshly prepared APS aqueous solutions of different concentrations. The resulting solution was stirred overnight at 500 rpm, and 22 °C, under a nitrogen purge. At the completion of polymerization, hexane was removed by rotary evaporation and the particles were resuspended by addition of ethanol (50 mL).

The processing and preservation of the obtained NPs were tested by numerous methodologies, such as ultracentrifugation, ultrasonication, dialysis and lyophilization. In order to keep these samples viable, they were kept in a refrigerator (4 °C) or freezer (−8 °C). Dynamic light scattering (DLS) was employed to determine the size of the NPs in aqueous solution.

2.4. Loading of nanoparticles with photosensitizers

13.7 μL of Tween-80 were added to 1.37 mL (10 mg) of NPs solution. Prior to loading, NR, NRBr, AzB and AzBBr were dissolved in DMSO to prepare 20 mM solutions. For loading, different aliquots of NR, NRBr, AzB and AzBBr were added to the NPs solution and magnetically stirred at a constant rpm for at least 2 h. The excess of DMSO, Tween 80 and NR, NRBr, AzB, AzBBr that were not loaded, was removed by dialysis (24 h). The supernatant was measured spectrophotometically until no absorbance for NR, NRBr, AzB and AzBBr was detected. The concentration of loaded dyes was measured spectrophotometrically in acetonitrile (NR and NRBr) and methanol (AzB and AzBBr) according to the Beer–Lambert law, using 30939.31 and 26092.06 ($L\,mol^{-1}\,cm^{-1}$) as the molar

Table 2
Polyacrylamide nanoparticles charged with PSs.

PS[a]	Aliquot (μL)	Loaded percentage (%)	Charged amount[b] (mg)
NR	200	99.1	0.7 (±0.1)
	400	98.5	1.7 (±0.2)
	600	88.4	2.0 (±0.4)
	800	80.1	2.5 (±0.5)
NRBr	200	87.4	0.4 (±0.1)
	400	95.7	0.8 (±0.2)
	600	98.4	1.6 (±0.3)
	800	91.5	2.2 (±0.2)
AzB	200	98.6	0.6 (±0.1)
	400	94.8	1.2 (±0.5)
	600	97.7	2.0 (±0.4)
	800	74.0	2.2 (±0.3)
AzBBr	200	99.9	0.6 (±0.1)
	400	98.4	1.2 (±0.4)
	600	98.5	1.5 (±0.3)
	800	98.9	2.5 (±0.7)

[a] Stock solution concentration: 20 mM.
[b] Constant amount of NP: 10 mg.

Table 1
Reaction conditions for prepared NPs.

Reaction Number	Time (h)	TEMED and APS (μL)	APS (% w/v)	Average Size (nm)	Zeta Potential (mV)	PDI
1	8	20	10	125	−35	0.28
2	8	35	10	130	−35	0.35
3	13	13.35	7	80	−30	0.20
4	13	13.35	10	100	−34	0.22
5	13	55	25	330	−33	0.26
6	15	35	25	165	−37	0.33
7	15	20	10	105	−32	0.30

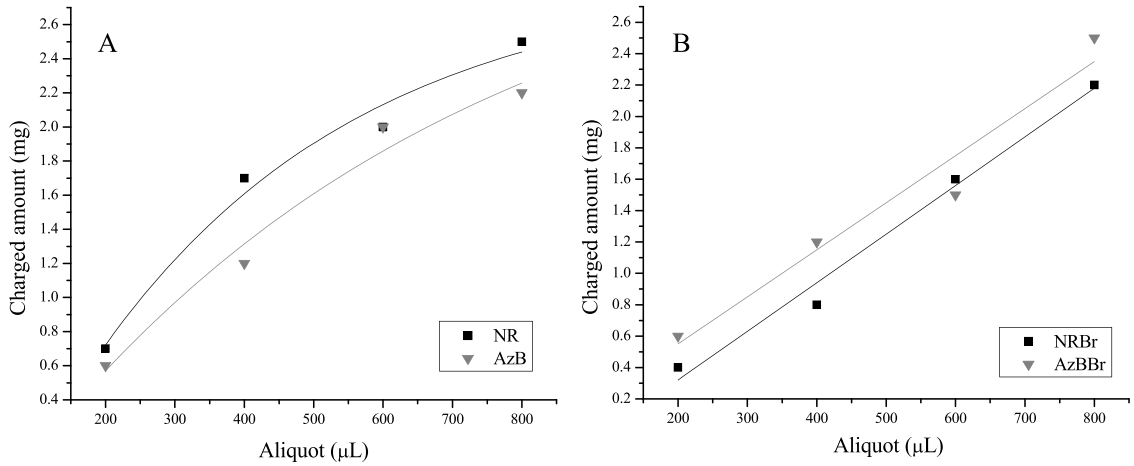

Fig. 3. PS amount loaded in the NPs as a function of the aliquot of the dye used in the charging process for commercial compounds (A) and new mono-brominated derivatives (B).

extinction coefficient for NR and NRBr, respectively, and 58370.01 and 38905.99 ($L\,mol^{-1}\,cm^{-1}$) for AzB and AzBBr, respectively.

2.5. Calibration curves, stock and preparations of standard solutions

Stock solutions of NR, NRBr and AZB, AzBBr (3.5×10^{-4} M) were prepared in acetonitrile (ACN) and methanol, respectively, prior to use. Standard solutions (5 mL) of these compounds were prepared by diluting different aliquots of the corresponding stock solution with ACN or methanol.

The calibration curves for NR, NRBr, AzB and AzBBr were obtained at ten different concentrations, equally distributed in the range from 7.5×10^{-6} to 4.5×10^{-5} M, 1×10^{-5} to 8×10^{-5} M, 2.5×10^{-6} to 2.5×10^{-5} M and 5.0×10^{-6} to 2.0×10^{-5} M, respectively. The slopes and intercepts were determined by the least-squares linear regression analysis method. The regression coefficients (r^2) were always higher than 0.9996.

2.6. Photodynamic properties: singlet oxygen determination

Solutions of NR, NRBr, AzB and AzBBr dyes were irradiated at 5 cm distance with a Parathom® lamp (OSRAM −5 W) in 1 cm path length quartz cells with ABDA (absorbance ~0.3) in Milli-Q water. To insure that an equal number of photons were absorbed per unit time in all experiments, the concentration for each dye was adjusted at an absorbance of ~0.20 at the λ_{max}. The kinetic of ABDA photooxidation was studied by following the decrease of the absorbance (Abs) at λ_{max} = 380 nm as a function of irradiation time (Fig. 2). The observed rate constants (k_{obs}) were obtained by a linear least-squares fit of the plot of Abs versus time and the values of singlet oxygen quantum yields (Φ_D) were calculated respect to the parent compound used as reference (NR, AzB, Φ_Δ = 1).

The Φ_Δ of the dyes were calculated using Eq. (1), where PS is the photosensitizer, Ref is the reference compound and Abs_0 is the initial absorbance of each PS at maximum absorption wavelengths.

$$\Phi_\Delta^{PS} = \frac{\Phi_\Delta^{Ref} k_{obs}^{PS} Abs_0^{Ref}}{k_{obs}^{Ref} Abs_0^{PS}} \quad (1)$$

2.7. Chemical stability studies

Stock solutions of free dyes and loaded NPs with NR, NRBr, AZB and AzBBr (5×10^{-4} M) were prepared in *buffer* pH 7.4 prior to use. Standard solutions (25 mL; 3.5×10^{-5} M) of these compounds were prepared by diluting different aliquots of the corresponding stock solution with *buffer* pH 7.4. Samples were placed in a thermostatic bath at 37 °C. Aliquots were taken at different times and their Abs values were measured. The study was conducted for 6 h.

3. Results and discussion

3.1. Synthesis and characterization of nanoparticles

Several parameters, such as reaction time, amount of APS and TEMED have been tested in order to obtain the desired NPs. Table 1 summarizes the most representative reaction conditions that allowed the selection of the optimal.

In accordance with the results obtained, it is possible to state that the increase in the amount of TEMED and APS increased the size of the NPs and PDI while the other parameters held constant. This arises from the comparison between reactions N° 5–6. Also, the addition of a more concentrated solution of APS allowed obtaining larger and polydisperse NPs (reactions 3–4). Finally, it was determined that the greatest reaction time slightly favored the formation of smaller NPs, which was important in the selection of the final reaction time. The in-depth analysis of these parameters allowed us to select the proper working methodology, as well as elucidate the optimum reaction conditions.

All NPs sizes were in the range of 80–330 nm, with PDI values around 0.20–0.35 and a zeta potential of −30 mV in most cases.

According to these results, it can be said that the conditions of the synthesis described in reaction N° 3 (Table 1), are optimal for the preparation of synthetic NPs since they allow obtaining systems with a size of 80 nm and acceptable PDI. These values allowed the conclusion that NPs are distributed in only one population and are similar in size (Lancheros et al., 2014). Also, the determined zeta potential value is indicative of high stability (Gupta and Kompella, 2006).

Regarding the processing and preservation, dialysis through special membranes 50 kDa (3 days) was selected, first in ethanol to remove the surfactant and residual monomers, and then in water (3 days). The samples purified by dialysis were stored in a refrigerator at 4 °C.

Table 3
Kinetic parameters for the photooxidation and Φ_Δ of loaded NR and NRBr inNPs.

PS in NPs	Absorbance	k_{obs} (x10^{-4}; s^{-1})	Φ_Δ
NR	0.285 ± 0.002	2.7 ± 0.1	1
NRBr	0.204 ± 0.004	4.0 ± 0.3	2.1

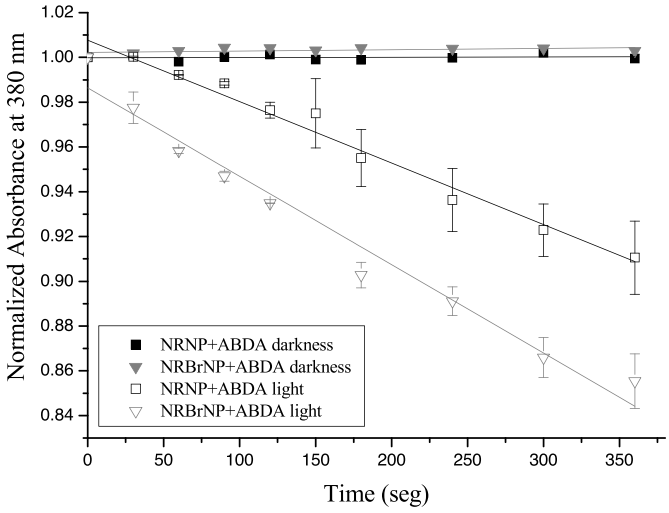

Fig. 4. Kinetics of ABDA photooxidation at λ_{max}=380 nm as a function of irradiation time for different PSs.

3.2. Loading of nanoparticles with photosensitizers

The results of the loading of NPs of polyacrylamide (PAA) with PSs are summarized in Table 2. According to these results, it is possible to state that in all cases the loading percentage remained between 80 and 99%. As for the family of phenazines (NR and NRBr), the loading percentage for the precursor NR decreased as the PS aliquot added to the NP increased. In contrast, the novel derivative (NRBr) showed, in general, a reverse behavior, that is, the loading efficiency was increased.

Regarding the phenothiazines (AzB and AzBBr), the precursor AzB exhibited a lower loading percentage as the aliquot of the added PS increased, which is similar to that reported for NR. However, for the new derivative (AzBBr), this result remained high and constant.

As shown in Fig. 3(A and B), the amount of the PS encapsulated in NPs increased with increasing concentration of PS at the initial stage of loading, reaching a maximum of 2 mg with an aliquot of 800 μL for all the studied PSs. It should be noted that NR and AzB showed an exponential behavior (Fig. 3A), reaching a constant maximum load value from 800 μL of the incorporated PS. On the other hand, monobromated derivatives (Fig. 3B) exhibited a linear tendency with the increase of the initial PS aliquot, without reaching the maximum load of the system.

This difference in the entrapment can be explained by the fact that the most hydrophobic dyes have limited water solubility. Some literature have reported that drug loading is strongly influenced by drug lipophilicity, where more lipophilic drugs exhibit higher encapsulation efficiency in numerous delivery systems (Cheow and Hadinoto, 2011; Pegaz et al., 2005). Since bromination causes an increase in the lipophilicity of these PSs, the NPs are expected to load a greater quantity of the new halogenated derivatives (Montes de Oca et al., 2013; Urrutia et al., 2015).

Table 4
Kinetic parameters for the photooxidation and Φ_Δ of free phenothiazine dyes in water and loaded in NPs.

PS	Absorbance	k_{obs} (x10^{-3}; s^{-1})	Φ_Δ
Free in H_2O			
AzB	0.161 ± 0.002	1.25 ± 0.03	1
AzBBr	0.195 ± 0.004	0.96 ± 0.02	0.63
Loaded in NPs			
AzB	0.138 ± 0.002	0.91 ± 0.02	1
AzBBr	0.249 ± 0.006	1.40 ± 0.05	0.85

3.3. Photodynamic properties: singlet oxygen determination

The values of the observed rate constant (k_{obs}) were obtained and Φ_Δ were calculated, using Eq. (1) (Tables 3 and 4).

According to the results obtained, the singlet oxygen yield for the PSs of the group of phenazines (NR and NRBr) was modified as follows: the new derivative (NRBr) increased twice the production of this oxygen species compared with that of the starting reagent (NR) when both were loaded in the NPs of the PAA (Table 3 and Fig. 4). This phenomenon is related to the "heavy atom effect", which leads to an increase in the photosensitizing effect (Zhao et al., 2013).

Furthermore, both PSs were better singlet oxygen generators when they were contained in the NPs than when they were present in aqueous solution (Fig. 4). Such behavior showed that the implementation of the NP system to deliver both PSs can be a promising alternative for drug formulation.

With regard to the group of phenothiazines (AzB and AzBBr), it can be said that the new derivative in aqueous medium exhibited a lower singlet oxygen yield compared with the starting reagent (Table 4). This may be because AzBBr in aqueous medium has a greater aggregation (dimer and trimer) than AzB. Possibly, this aggregate formation decreases the photodynamic efficacy of the phenothiazines. Therefore, it was predictable that the effectiveness of AzBBr in water would be similar or lower respect to AzB (Vara and Ortiz, 2016).

On the other hand, such PSs (AzB and AzBBr) in presence of NPs showed a similar behavior to that previously described. However, note that AzBBr in NPs displayed a greater singlet oxygen yield than the free compound in water. This demonstrated that the delivery of AzBBr increased its photodynamic efficiency, which is very favorable.

3.4. Chemical stability studies

Stability studies were carried out using both free and loaded dyes. According to the results obtained in our study, it can be stated that for the free dyes, NR, AzB, AzBBr did not show degradation in buffer pH 7.4 for 6 h (Data not shown). However, NRBr was very unstable (half-time ($t_{1/2}$) 10 min) (Fig. 5), and followed a pseudo-first order kinetics. This fact means that this pH affects the stability of NRBr.

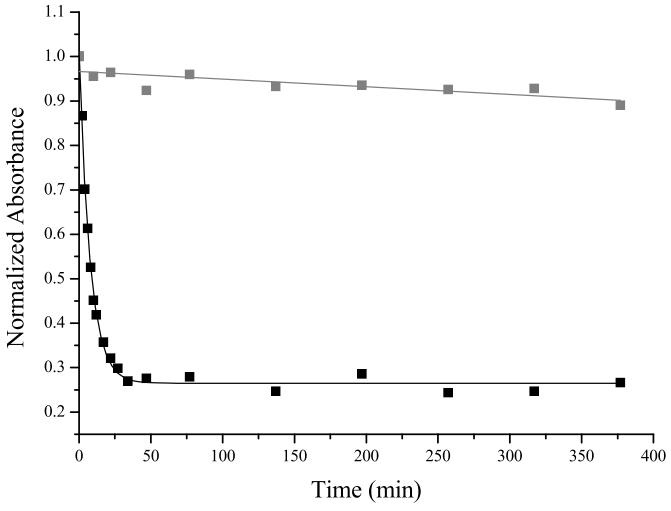

Fig. 5. Stability studies of free NRBr in water (■) and charged NRBr in NPs (■).

When the studies were performed in presence of the NPs of PAA, the stability of the NRBr compound increased significantly (It was stable during the 6 h study period, Fig. 5), which is advantageous for this drug. Similarly, NR, AzB and AzBBr remained stable.

The significant increase in the stability of NRBr can also be related to the increase in the singlet oxygen yield of this compound (see the section on photodynamic properties: singlet oxygen determination), which could be interesting in terms of a better biological activity of this new derivative since it is an essential property for the development of therapeutic agents.

4. Conclusion

In conclusion, we have described a novel method for the synthesis of PAA NPs. Acrylamide and APMA have been employed as monomers and AHM as the crosslinker. Several parameters have been considered in order to optimize the NPs synthesis. NPs have been characterized by DLS, showing the presence of particles with sizes of 80 nm.

Finally, we analyzed drug loading, the ability to generate singlet oxygen and chemical stability. The NPs described in this work presented ideal sizes and polydispersities, as well as good physicochemical properties. They are therefore envisioned as attractive delivery systems for the controlled release of different drugs. Besides, the entrapment of PSs offers therapeutic advantages in comparison to free PSs active agent since it prevents different adverse effects (degradation, aggregation, etc.). The novel NPs can be useful nanocarriers for poorly-water soluble phenazine and phenothiazine dyes as a novel third generation of photosensitizing agents used in photodynamic therapy since this system can tailor the physicochemical characteristics of the final NPs.

Acknowledgments

This work was supported by grants from Secretaría de Ciencia y Técnica (SeCyT)203/2014; 103/2015 and Fondo para la Investigación Científica y Tecnológica (FonCyT). MSG and JV gratefully acknowledge receipt of a fellowship from the Consejo Nacional de Investigaciones Científicas y Técnicas (CONICET).

References

Alvarez, M.G., Montes de Oca, M.N., Milanesio, M.E., Ortiz, C.S., Durantini, E.N., 2014. Photodynamic properties and photoinactivation of *Candida albicans* mediated by brominated derivatives of triarylmethane and phenothiazinium dyes. Photodiag. Photodyn. Ther. 11, 148–155.

Cheow, W.S., Hadinoto, K., 2011. Factors affecting drug encapsulation and stability of lipid–polymer hybrid Nanoparticles. Colloid Surf. B 85, 214–220.

Ferreira dos Santos, C., Sousa Gomes, P., Almeida, M.M., Willinger, M.G., Franke, R.P., Fernandes, M.H., 2015. Gold-dotted hydroxyapatite nanoparticles as multifunctional platforms for medical applications. RSC Adv. 5, 69184–69195.

Fischer, B.B., Krieger-Liszkay, A., Eggen, R.I.L., 2005. Oxidative stress induced by the photosensitizers neutral red (type I) or rose bengal (type II) in the light causes different molecular responses in *Chlamydomonas reinhardtii*. Plant Sci. 168, 747–759.

Gupta, R.B., Kompella, U.B., 2006. Nanoparticle Technology for Drug Delivery. Taylor and Francis Group, New York.

Kolya, H., Tripathy, T., 2014. Biodegradable flocculants based on polyacrylamide andpoly(N,N-dimethylacrylamide) grafted amylopectin. Int. J. Biol. Macromol. 70, 26–36.

Lancheros, R.J., Beleño, J.A., Guerrero, C.A., Godoy-Silva, R.D., 2014. Producción De Nanopartículas De PLGA Por El método De Emulsión Y Evaporación Para Encapsular N-Acetilcisteina (NAC), 19. Universitas Scientiarum, pp. 161–168.

Li, L., Huh, K.M., 2014. Polymeric nanocarrier systems for photodynamic therapy. Biomater. Res. 18–19, 1–14.

Master, A., Livingston, M., Sen Gupta, A., 2013. Photodynamic nanomedicine in the treatment of solid tumors: perspectives and challenges. J. Control. Release 168, 88–102.

Maya, S., Sarmento, B., Amrita, N., Sanoj Rejinold, N., Shantikumar, V.N., Jayakumar, R., 2013. Smart stimuli sensitive nanogels in cancer drug delivery and imaging: a review. Curr. Pharm. Design. 19, 7203–7218.

Montes de Oca, M.N., Vara, J., Milla, L., Rivarola, V., Ortiz, C.S., 2013. Physicochemical properties and photodynamic activity of novel derivatives of Triarlylmethane and Thiazine. Arch. Pharm. Chem. Life Sci. 346, 255–265.

Paszko, E., Ehrhardt, C., Senge, M.O., Kelleher, D.P., Reynolds, J.V., 2011. Nanodrug applications in photodynamic therapy. Photodiagn. Photodyn. 8, 14–29.

Pegaz, B., Debefve, E., Borle, F., Ballini, J.P., van den Bergh, H., Kouakou-Konan, Y.N., 2005. Encapsulation of porphyrins and chlorins in biodegradable nanoparticles: the effect of dye lipophilicity on the extravasation and the photothrombic activity. A comparative study. J. Photochem. Photobiol. B. 80, 19–27.

Pereira Rosa, L., da Silva, F.C., Alves Nader, S., Andrade Meira, G., Souza Viana, M., 2015. Antimicrobial photodynamic inactivation of *Staphylococcus aureus* biofilms in bone specimens using methylene blue, toluidine blue ortho and malachite green: an in vitro study. Arch. Oral Biol. 60, 675–680.

Rodrigues, G.B., Dias-Baruffi, M., Holman, N., Wainwright, M., Braga, G.U.L., 2013. In vitro photodynamic inactivation of *Candida* species and mouse fibroblasts with phenothiazinium photosensitisers and red light. Photodiagn. Photodyn. 10, 141–149.

Saha, D., Hosen, S.M.Z., Paul, S., 2015. Pharmaceutical nanotechnology: strategies and techniques of drug therapy: disease and delivery through pharmaceutical biotechnology. Univ. Mauritius Res. J. 21, 1–17.

Singh, M.K., Pal, H., Bhasikuttan, A.C., Sapre, A.V., 1999. Photophysical properties of the cationic form of neutral red. Photoch. Photobio. 69, 529–535.

Swarnalatha Lucky, S., Chee Soo, K., Zhang, Y., 2015. Nanoparticles in photodynamic therapy. Chem. Rev. 115, 1990–2042.

Urrutia, M.N., Ortiz, C.S., 2013. Spectroscopic characterization and aggregation of azine compounds in different media. Chem. Phys. 412, 41–50.

Urrutia, M.N., Alovero, F.L., Ortiz, C.S., 2015. New azine compounds as photoantimicrobial agents against *Staphylococcus aureus*. Dyes Pigm. 116, 27–35.

Vara, J., Ortiz, C.S., 2016. Thiazine dyes: evaluation of monomeric and aggregate forms. Spectrochim. Acta A 166, 112–120.

Weijer, R., Broekgaarden, M., Kos, M., van Vught, R., Rauws, E.A.J., Breukink, E., 2015. Enhancing photodynamic therapy of refractory solid cancers: combining second-generation photosensitizers with multi-targeted liposomal delivery. J. Photochem. Photobiol. C 23, 103–131.

Yano, S., Hirohara, S., Obata, M., Hagiya, Y., Ogura, S., Ikeda, A., 2011. Current states and future views in photodynamic therapy. Photochem. Photobiol. C 12, 46–67.

Yuri Nagata, J., Hioka, N., Kimura, E., Batistela, V.R., Suga Terada, R.S., Graciano, A.X., 2012. Antibacterial photodynamic therapy for dental caries: evaluation of the photosensitizers used and light source properties. Photodiagn. Photodyn. 9, 122–131.

Zhao, J., Wu, W., Sun, J., Guo, S., 2013. Triplet photosensitizers: from molecular design to applications. Chem. Soc. Rev. 42, 5323–5351.